Available online at www.sciencedirect.com

ScienceDirect

Materials Today: Proceedings XX (2016) XXX–XXX

materialstoday: PROCEEDINGS

www.materialstoday.com/proceedings

PMME 2016

Analysis of hole expansion limit through biaxial test*

Chetan P Nikhare*

Mechanical Engineering, Penn State Behrend, Erie, PA – 16563, USA

Abstract

Predicting failure of a material is one of a challenge in the metal forming area. Also advancement of a material for higher strength and ductility could not be achieved without bringing the complexities at the micro level. This complexity at the micro level is due to the multi phases in a material. Due to which it creates the heterogeneity in a material which hugely affects the mechanical behaviour and creates a challenge on determining the limits of the material and their failure characteristics. In this paper hole expansion technique is investigated to observe the limits of a material. Hole expansion process is one of the material mechanical characterization method which provides the material edge characteristics during forming/stretching. The specimen used in this process was cruciform shape with hole at the centre. The specimen arms were then pulled to create the three deformation modes i.e., uniaxial, plane strain and biaxial. The strain evolution for the critical element in all three deformation modes was analysed. Also the hole expansion was monitored for the whole process. From the results it was observed that the critical element predicts the forming limit however hole expansion predicts the fracture behaviour of the material and found one of the useful tool to predict the fracture limit.

Selection and Peer-review under responsibility of International Conference on Processing of Materials, Minerals and Energy (July 29th – 30th) 2016, Ongole, Andhra Pradesh, India.

Keywords: Hole expansion, forming limit curve, biaxial test, hemispherical dome test, numerical simulation

* Corresponding author. Tel.: +1-814-898-7588; fax: +1-814-898-6125.

E-mail address: cpn10@psu.edu

Selection and Peer-review under responsibility of International Conference on Processing of Materials, Minerals and Energy (July 29th – 30th) 2016, Ongole, Andhra Pradesh, India.

1. Introduction

Across the board, investigators are struggling on how to provide efficient design which would meet the requirement for stricter environmental regulation. These environmental regulations and cost of fuel drives the need for lighter weighing, compactly designed vehicle parts. Due to light weight the mileage on the vehicle increases and can see a direct cost savings. This need has steadily increased due to recent economic changes and put automakers in the upmost position to think on efficient design which would lead for more savings by reducing the material waste, efficient use of material and energy. One of the ways on which many researcher are working is the efficient use of material i.e., either use higher density material with higher deformation of use lower density material which basically lacks deformation. In both case the deformation is one of the challenge which needs to address and understand properly for efficient design.

To understand the deformation closely in various modes, the forming limit diagram is one of the useful and powerful tools. This diagram is a plot between major and minor strain on a plane of sheet metal. This provides the indication on how, when and where the material will reach to failure and prevention technique to stop the deformation. Keeler [1] was the one who proposed the concept of forming limit curve on the major and minor axis of strain i.e., strain plane. This was further experimented on sheet metal during various stamping modes [2]. This forming limit curve provides a curve or envelope by joining limits in various tensioned modes. Basically this envelope floats from uniaxial to biaxial strain direction. Strain point above the envelope indicates the material failure by necking or tearing and point below refers to safety of a material [3]. It was identified in these literature [4-13] that this envelope is very sensitive to these parameters a) planar and normal anisotropy value “r-values”, b) strain hardening exponent “n-value”, c) strain rate “ε/sec-value”, d) size of grain at start of deformation, e) prestrain, f) tool geometry, g) coefficient of friction between sheet metal and tool, and h) blank holding force. Traditionally hemispherical dome tests were used to identify the limits of the material in various deformation modes. Primarily to determine the limits in the forming, the sheet metal was etched with the circle grids and then the metal gets stretched till neck/failure. The major and minor strain of a circle, which is near to a neck, or failure circle was measured and considered as a limit for that deformation mode. However in some process (like spin forming or single or double point incremental forming) the material gets stretched to extreme limit locally and does not get predictable with the conventional limit curve [14-17]. To accurately predict the limit in these cases the necking or fracture limit curve needs to determine. Researchers have applied multiple ways to determine these fracture limit curve, one of them is to measure the fracture thickness strain and then determine the major strain, considering the minor strain does not change after neck [18]. Other approach is to use the digital image correlation camera, but as soon as the necking appears the paint fall off and makes hard to read the strain.

A new testing method called biaxial test was devised, which can deform the material in various modes similar to traditional method with elimination of contact conditions. For this study the experimental testing previously performed on the Penn State Behrend’s newly developed high-capacity biaxial machine was considered. The sample used for this test rig is the cruciform shape samples which has 4 arms which can be displaced in positive direction to get various deformation modes. The hole was drilled at the center part of the sample to understand the post necking behavior. The specimen is simulated till its failure in the biaxial set-up. The critical element was then analyzed and compared with conventional forming limit diagram. Further the hole deformation was analyzed and superimposed with the forming limit. The noted differences were detailed and explained.

2. Material

To perform this study aluminum alloy 5083 was considered. The as-received material was brittle in nature and thus annealing operation at 500^{o}C for 5 minutes was performed to increase the ductility [19]. The tensile true stress strain for this annealed material is shown in Fig. 1. The tensile behavior was further fitted with power law and parameters were used for numerical simulation with isotropic hardening. However initial part of the yielding was directly included for the actual test. The mechanical properties of this annealed material are given in Table 1.

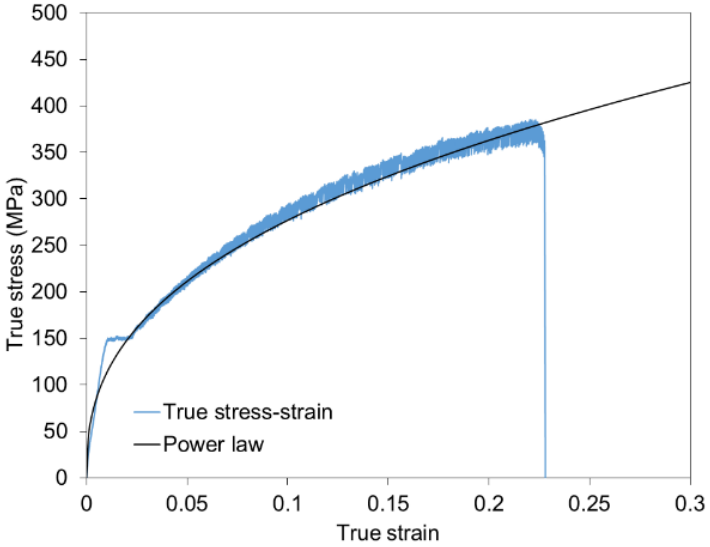

Fig. 1. True stress strain curve along with fitted power law [20]

Table 1. Mechanical properties of annealed AA5083 as determined by testing [20]

Yield Stress (MPa)	Tensile Stress (MPa)	Elongation (%)	K (MPa)	n
150	290	26	680	0.39

3. Numerical Methodology

The sample dimension used for this study is shown in Fig. 2. The cruciform specimen shape as shown in the figure was used for this work. 10 mm diameter hole was created at the center of the cruciform specimen and used for hole expansion simulation. ABAQUS/Explicit 6.13-2 simulation software was used to simulate the hole expansion process. The material tensile data as mentioned above was inputted in the numerical model with isotropic hardening law. In this work the specimen was stretched in 3 deformation mode 1) Uniaxial, 2) Plane strain and 3) Biaxial. To model these three conditions, the arm outer edges as shown in Figure 3 were controlled by displacement. The displacements were provided in such a way that the hole will always be at the center in the space. For uniaxial deformation mode only displacement 1 and 2 were provided and boundary condition on edge 3 and 4 were kept motion free. For plane strain condition the edges 3 and 4 were kept fixed and for biaxial condition all edges were allowed with same positive displacement. Three dimensional (Fig. 3a) was used to model these tests. The specimen was kept as a deformable body with S4R (4 node quadrilateral, reduced integration) shell elements. Finer mesh was applied at the hole and arm (Fig. 3b). Five integration points through the thickness direction were used to accurately predict the thinning and necking.

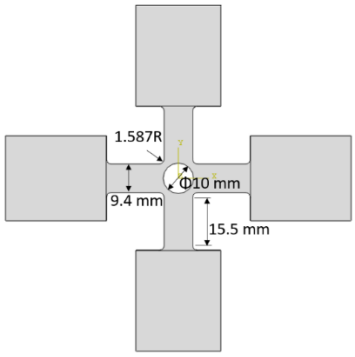

Fig. 2. Cruciform specimen with center hole [20]

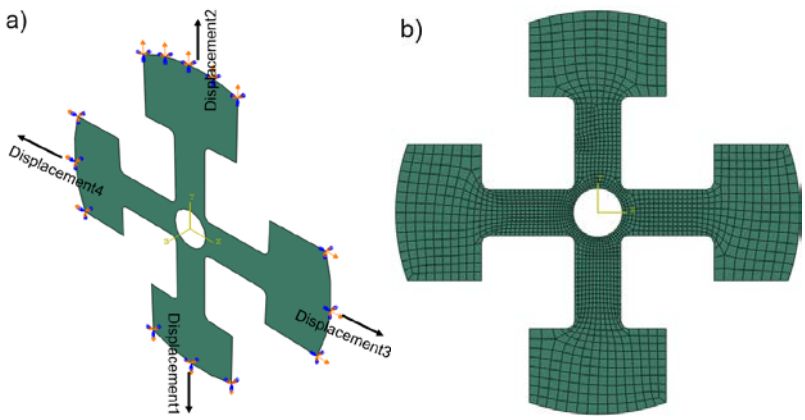

Fig. 3. Cruciform specimen numerical model a) with boundary condition and b) meshed specimen

4. Results and discussion

4.1. Validation of model with previous data

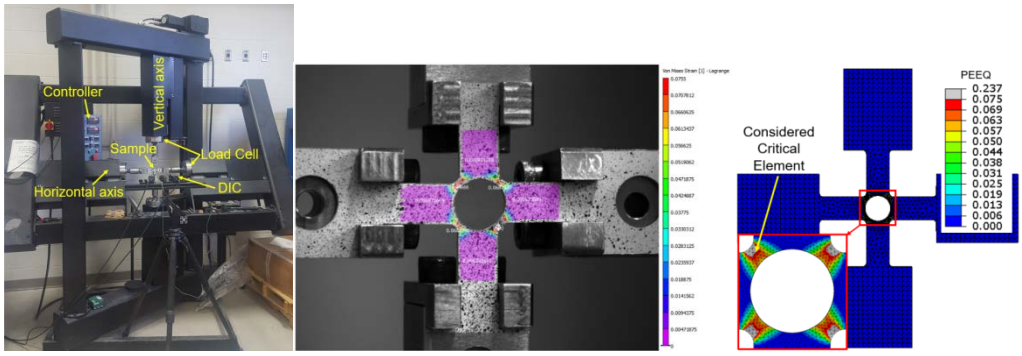

Fig. 4. Biaxial test: experimental set-up (left), deformed specimen near to failure (centre), and numerically deformed specimen (right) [20]

Figure 4 (left) shows the experimental set-up for biaxial test on NSF funded biaxial machine. The horizontal and vertical axes can set in a way that the multiple deformation modes can be achieved. Previous experiments were performed on the non-annealed specimens of AA5083 material in a biaxial deformation mode. The strain evolution

was captured with digital image correlation and discussed in more detail in this literature [20]. Figure 4 (centre) shows the equivalent strain in the specimen during loading condition at the start and near to failure. This was then modeled in ABAQUS and results were captured closely in agreement with the experiments as shown in Fig. 4 (right) [20].

4.2. Hole expansion in uniaxial, plane strain and equi-biaxial deformation mode

With the knowledge of proven numerical model, the simulations were set-up in a similar fashion with shell elements for uniaxial, plane strain and biaxial deformation mode for this study. Figure 5 shows the simulated specimen in respective deformation mode at the verge of failure. It can be observed that the most strained element in the uniaxial deformation mode is at the top edge of the corner radius and it shifts towards the radius center for plane strain and at the radius center for equi-biaxial mode.

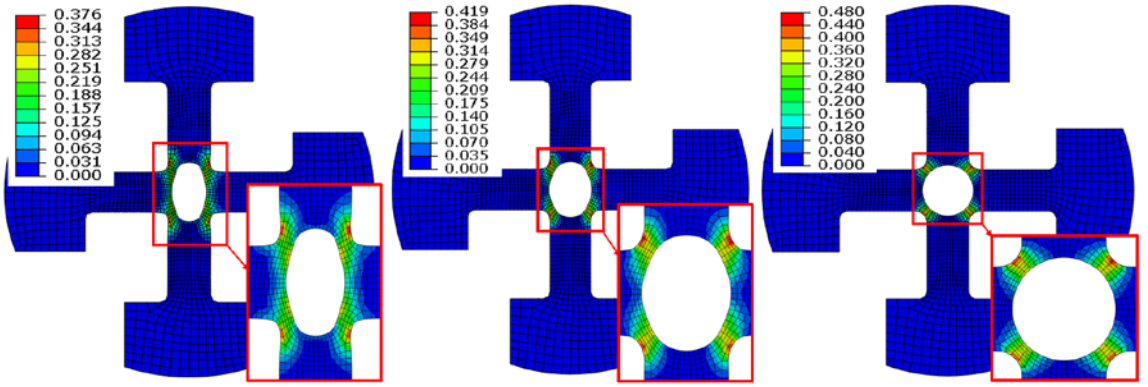

Fig. 5. Simulated specimen showing the verge of failure in uniaxial (left), in plane strain (centre), and in biaxial (right)

4.3. Hemispherical dome test data

The major strain of the critical element in all three deformation modes are plotted in Figure 6 (left). It is noted that as soon as the material would fail the major strain rises suddenly. The deviation of the strain (black circles in the figure) with respect to simulation time was considered as a failure point. The major strain is always positive in all deformation modes and can be observed from the figure. Figure 6 provides the minor and the thickness strain with respect to simulation time. The minor strain will be negative in the uniaxial deformation mode, almost zero in plane strain and positive in biaxial mode as was captured by the model nicely. Further Fig. 6 (right) provides the negative strain in all deformation mode as in all case the thickness will decrease due to stretching perpendicular to the thickness plane.

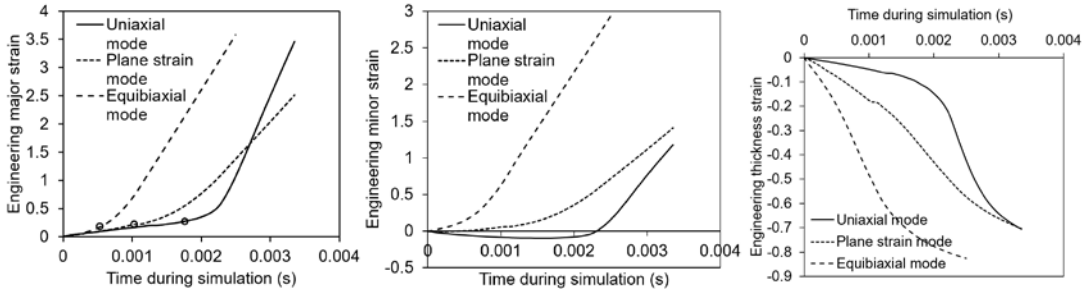

Fig. 6. Strain with respect to time: major (left), minor (centre), and thickness (right)

To observe the strain evolution in an element with respect to the hole Fig. 7 plots the major and minor strain of the hole during simulation in uniaxial, plane strain and equi-biaxial deformation mode. It was noted that the deviation occurs at different simulation time as for the element. Again the deviation point is considers as the saturation of hole expansion and contraction if any in that deformation mode. However, the deviation cannot be seen in the equi-biaxial deformation mode is because both horizontal and vertical arms are pulling at same rate and only the radius part realizes the failure and other part remains un-stretched after some point.

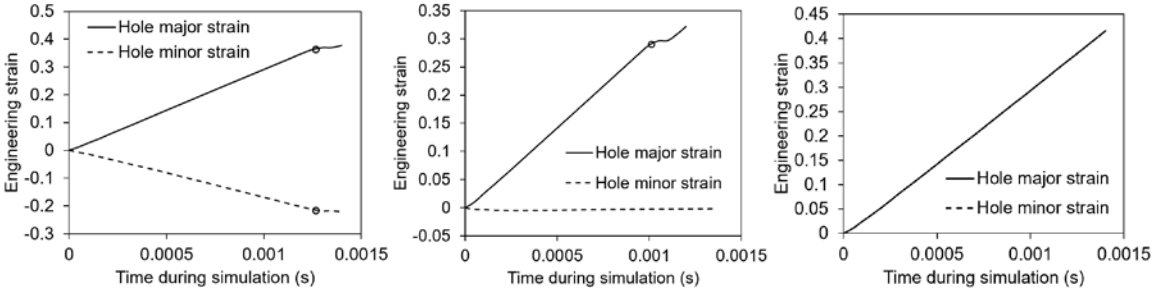

Fig. 7. Hole expansion and contraction with respect to time in uniaxial (left), plane strain (centre), and biaxial (right)

As the deviation point differs on how the element is stretched than the hole, it is worth plotting the strain path and the forming limit curve of the material. Figure 8 provides the expansion of hole in uniaxial, plane strain and equi-biaxial deformation mode. Further the forming limit curve of the base material [21] was referred and shifted for annealed condition based on how the deviation for failure was occurred [19, 22] and plotted. Further based on the deviation of the hole expansion the another limit was plotted and this can be considered as the hole failure/separation limit. With this observation, it can be noted that this procedure can provide a useful tool to predict the forming and the fracture/separation limit of a material.

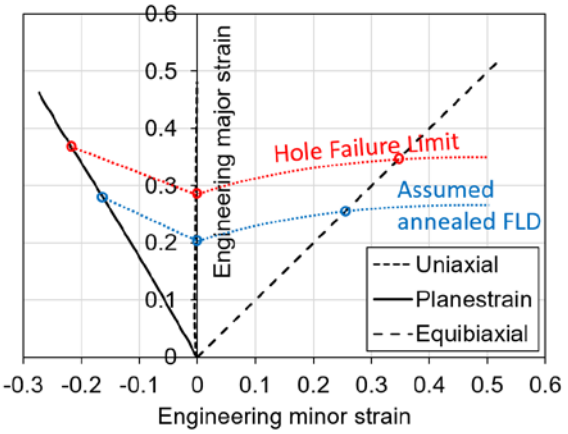

Fig. 8. Hole failure with respect to FLD

5. Conclusion

In this work the hole was expanded in three main deformation modes i.e., uniaxial, plane strain and equi-biaxial. For this the cruciform shape specimen was used with a center hole of 10 mm. The specimen arms were conditioned to pull such that the three deformation modes can be created. The specimens were stretched till failure and were identified through the deviation of strain path method. It was noted that the critical region was at the end of radius between the arms in uniaxial deformation mode and shift towards the center of radius for plane strain and right at the center of radius in equi-biaixal mode. It was also observed that the strain with respect to time of simulation starts

deviating as soon as the instability of an element occurred. With further analysis of the hole expansion it was found that the actual strain of a hole failure delayed as what was observed for the element failure. On plotting both instability limits it was found that the limit for actual hole expansion is higher than the element limit. This information provides us the knowledge that even if the element is neck the hole is not failed but on the way of failure and can be considered as a fracture limit of a material. However the complete validity is not been carried out and can be analyze through experiments in future. However it can be concluded that instead of using conventional method of fracture thickness measurements to predict the fracture limit hole expansion tool would be the preferred and easier to determine fracture limit.

Acknowledgements

The author would like to acknowledge National Science Foundation biaxial equipment funding CMMI – 1100356 and Penn State Erie, the Behrend College for providing research resources and thanks to technician Mr. Glenn Craig for fabrication of tests samples.

References

[1] S.P. Keeler, Sheet Metal Industries 42 (1965) 683–691.
[2] G.M. Goodwin, Sheet Metal Industries 60 (1968) 767–774.
[3] C. Nikhare, Y. Korkolis, and B.L. Kinsey, International Deep Drawing Research Group Conference, Mumbai, India (2012).
[4] R. Sowerby, J.L. Duncan, International Journal of Mechanical Sciences 13 (1971) 217–229.
[5] A.K. Ghosh, S.S. Hecker Metallurgical Transaction A 5A (1974) 1607– 1616.
[6] F. Stachowicz, Journal of Mechanical Working Technology 19 (1989) 305–317.
[7] A. Graf, W. Hosford, Metallurgical Transactions A 24A (1993) 2503-2512.
[8] R. Arrieux, Annals of CIRP 36 (1987) 195-198.
[9] R. Arrieux, C. Bedrin, M. Boivin, International Deep Drawing Research Group Conference (1982).
[10] Y.P. Korkolis, and S. Kyriakides, International Journal of Plasticity 25 (2009) 2059-2080.
[11] K. Yoshida, T. Kuwabara, K. Narihara, and S. Takahashi International Journal of Forming Processes 8 (2005) 283-298.
[12] A. Barata Da Rocha, F. Barlat, J.M. Jalinier Materials Science and Engineering 68 (1984) 151–164.
[13] C. Nikhare, R.A.C. Filho, L.M.V. Tigrinho, P.V.P. Marcondes, International Deep Drawing Research Group Conference, Mumbai, India (2012).
[14] J.M.C. Soeiro, C.M.A. Silva, M.B. Silva, P.A.F Martins, Journal of Materials Processing Technology 217 (2015) 184-192.
[15] M.B. Silva, K. Isik, A.E. Tekkaya, A.G. Atkins, P.A.F. Martins, Journal of Materials Processing Technology 234 (2016) 249-258.
[16] M.B. Silva, A.J. Martinez-Donaire, G. Centeno, D. Morales-Palma, C. Vallellano, P.A.F. Martins, Procedia Engineering 132 (2015) 342-349
[17] B. Ma, Z.G. Liu, Z. Jiang, X. Wu, K. Diao, M. Wan, Materials & Design 96 (2016) 401-408.
[18] C. Nikhare, M. Weiss, P.D. Hodgson, Materials Science and Engineering A 528 (2011) 3010-3013.
[19] C.P. Nikhare, E. Vorisek, J. Nolan and J.T. Roth, International Mechanical Engineering Congress and Exposition Conference, Phoenix, Arizona, United States (2016).
[20] C. Nikhare, J. Nolan, International Deep Drawing Research Group Conference, Linz, Austria (2016).
[21] F. Zhalehfar, R. Hashemi, and S.J. Hossenipour, International Journal of Advance Manufacturing Technology 76 (2015) 1343-1352.
[22] C. Nikhare, Numerical analysis on the effect of thickness on biaxial tension limits International Conference on Processing of Materials, Minerals and Energy (2016).